American Journal of Chemistry 2021, 11(1): 8-17
DOI: 10.5923/j.chemistry.20211101.02

Synthesis and Characterization of Nickel Doped Titanium Dioxide Nano Crystals Composite for the Treatment of Tannery Dye Wastewater

Amana B. S.[1,*], A. Giwa[2], H. R. Saliu[2], Ayebe B.[1], S. F. Tanko[1], J. D. Putshaka[3]

[1]Nigerian Institute of Leather and Science Technology (NILEST), Zaria
[2]Department of Polymer and Textile Engineering, Ahmadu Bello University, Zaria
[3]Nigerian Institute of Leather and Science Technology (NILEST), Jos Extension Centre

Abstract Nickel doped Titanium dioxide nanocrystals composite was synthesized via wet-impregnation method for 0.5%, 1%, 1.5% and 2% Ni-TiO_2 and characterized using X-ray diffraction pattern (XRD), X-ray florescence (XRF), Scanning Electron Microscopy (SEM) and band gap energy. The XRD results reveal that the phase structure of the synthesized samples was mainly in pure anatase phase having crystalline size in the range of 7nm-11nm, spherical shapes with moderate aggregation of the crystal particles were observed under the SEM, the XRF gives the exact percentage dopant in Ni-TiO_2 nano-crystal and the band gap energy was lowered from 3.1ev-2.95ev. The presence of the $NiNO_3$ at TiO_2 site has not only affected the nano-crystals morphologically but also induce the electronic property of the TiO_2 by lowering the band gap energy from 3.1ev-2.95ev which prone the decolouration of organic pollutants. The photocatalyst synthesized was found to effective in the mineralization of dye wastewater under visible light irradiation.

Keywords Nanocrystal, Wet-impregnation, Nickel, Titanium dioxide, Dye waste water

1. Introduction

Effluent being generated from synthetic dyes cannot be effectively treated using conventional processes due to their recalcitrant nature and are therefore candidates for Advanced Oxidation Processes (AOPs) [Han *et al.;* 2009, Martı´nez and Brillas, 2009]. AOPs is capable of mineralizing a wide variety of organic pollutants [O ¨ zcan *et al.;* 2009, Arshlan-Alaton, 2007; Rivas *et al.;* 2012, Forgacs *et al.;* 2004, Gomathi *et al.;* 2009] and Photocatalysis using metal doped Titanium dioxide has been widely reported as a promising technology for the removal of various organic and inorganic pollutants from wastewater and air because of its stability, low cost and non toxicity [Liu *et al.;* 2008, Zheng *et al.;* 2015]. Metal doped Titanium dioxide photocatalyst has consumed a great attention due to its enhanced photocatalytic activity at Visible region [Ganesh *et al.;* 2012, Yan-Hue *et al.;* 2012] and their wide band gap limits their photocatalytic activity in the ultraviolet region that contributes 3-5% of the total solar spectrum [Zheng *et al.;* 2015, Pouran *et al.;* 2016]. Nickel doped Titanium dioxide can therefore improved the visible responsive activity in environmental organic pollutant degradation through the utilization of solar energy [Visinescu *et al.;* 2015, Ahmed; 2012, Ahmed *et al.;* 2018]. This research focuses on Synthesising a Nickel doped Titanium dioxide that can utilized solar/electrical energy for the treatment of Tannery wastewater.

* Corresponding author:
amanaskido@gmaill.com (Amana B. S.)
Received: Jan. 15, 2021; Accepted: Jan. 30, 2021; Published: Feb. 6, 2021
Published online at http://journal.sapub.org/chemistry

2. Preparation of Ni-doped TiO_2

19.69 g of commercially available TiO_2 was dissolved in 100ml of distilled water and 0.31 g of $NiNO_3$ was then added to synthesize 0.5% Ni doped TiO_2. The mixture was then stirred at room temperature for 4 hrs continuously and the powder was separated by decantation. The supernatant liquid was then discarded and dried in an oven at 100 ℃ for 3 hrs and calcined for 4 hrs at 300 ℃ and crushed manually in the form of very fine powder. Similarly, 1.0, 1.5 and 2.0% Ni-TiO_2 were prepared only by changing the amount of $NiNO_3$ to 0.62g, 0.93g, 1.24g and that of Titanium dioxide mass to 19.38, 19.07, 18.76 to obtain Ni-TiO_2 in total mass of 20g respectively.

3. Result and Discussion

3.1. XRD Patterns of the Synthesized Ni-TiO_2 Catalyst

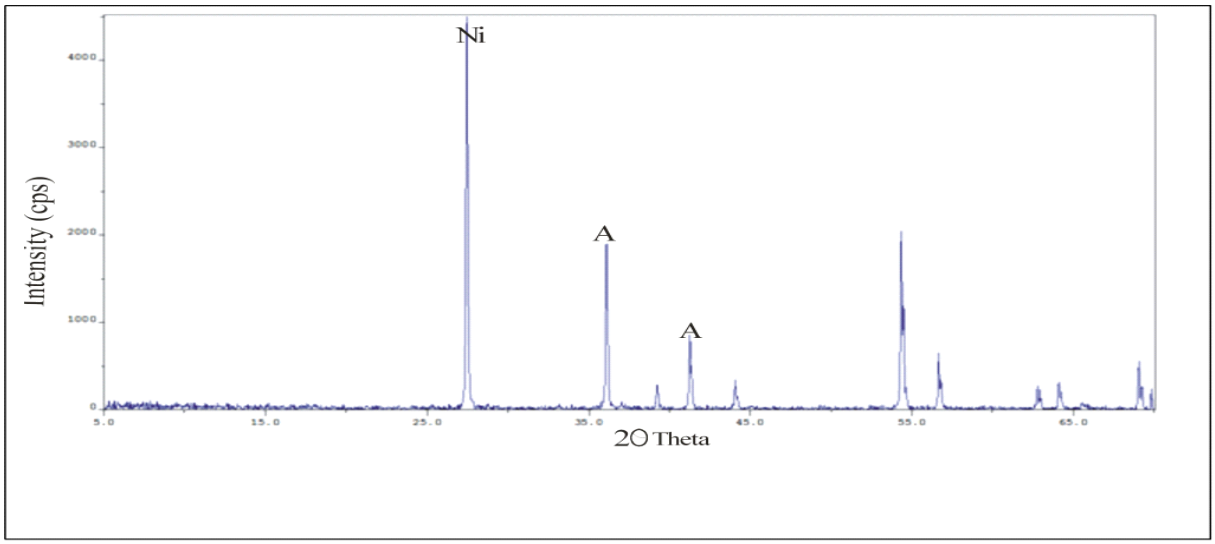

Figure 1a. XRD pattern for 0.5% Ni-TiO_2

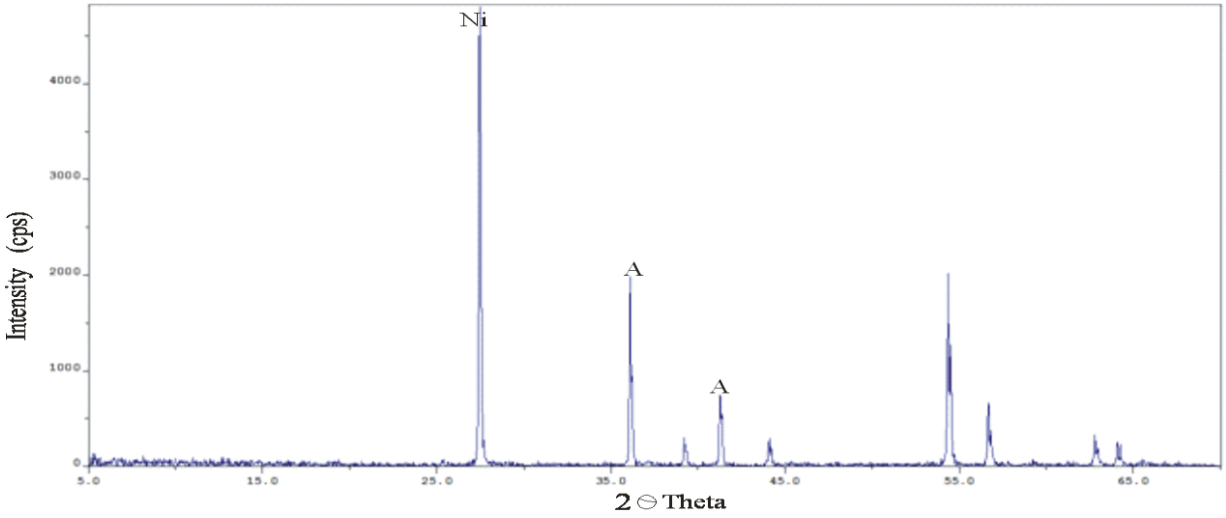

Figure 1b. XRD pattern for 1% Ni-TiO_2

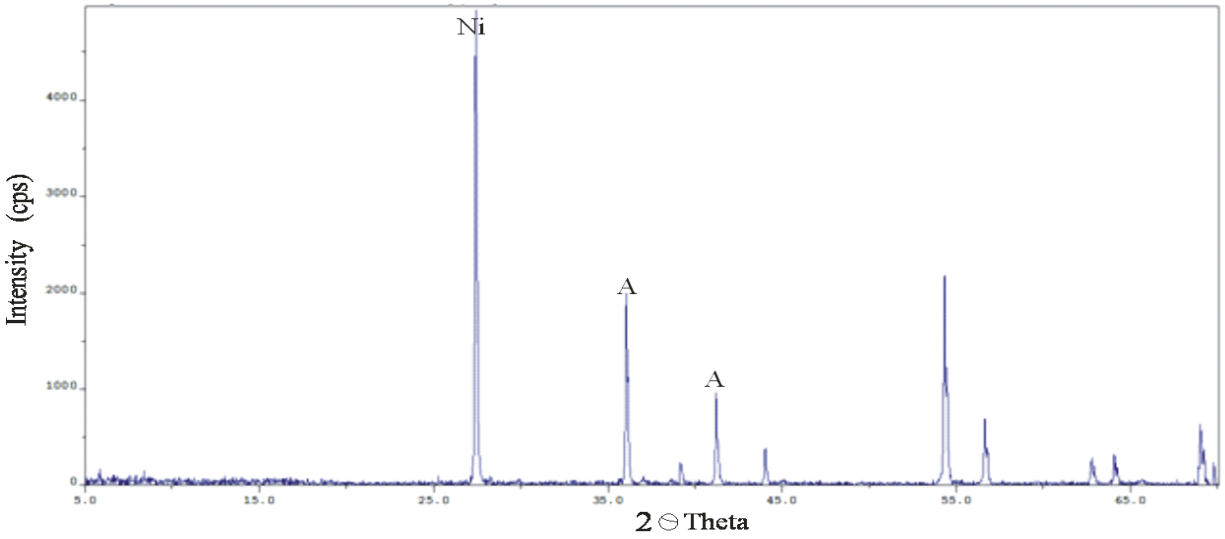

Figure 1c. XRD pattern for 1% Ni-TiO_2

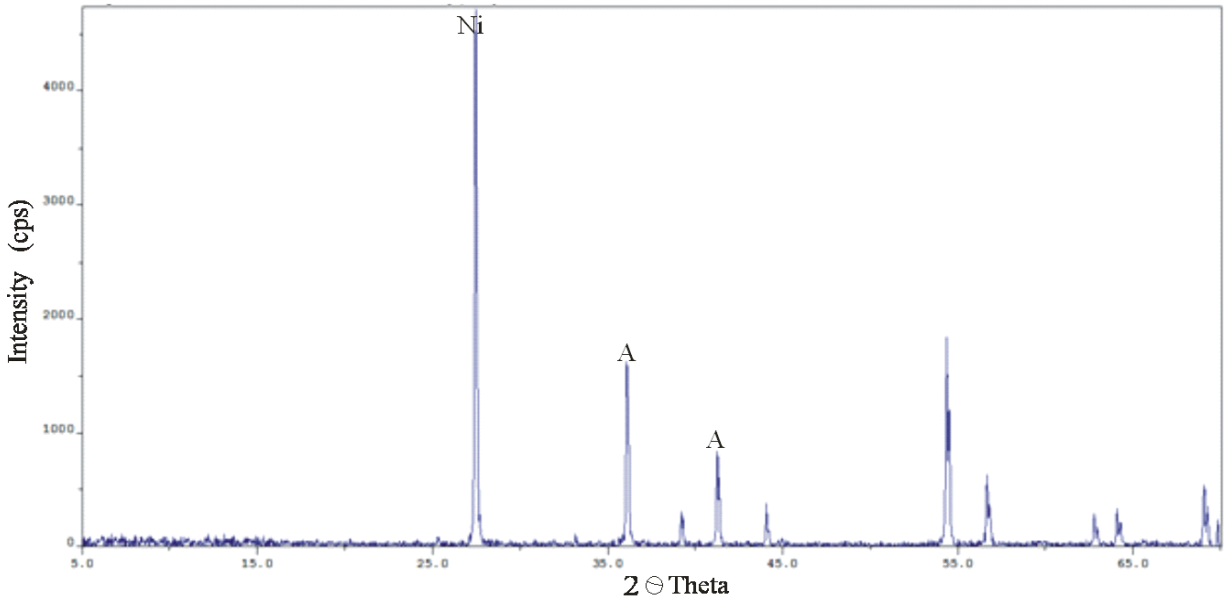

Figure 1d. XRD pattern for 1% Ni-TiO_2

Figure 1a, 1b, 1c and 1d shows the X-ray diffraction (XRD) pattern of 0.5%, 1%, 1.5% and 2% Ni-TiO_2 photocatalyst that is synthesized by wet impregnation method and the peaks are perfectly indexed as anatase phase. The average crystalline sizes was calculated from the sharer equation as 7.5nm compare with 0.5% Ni-TiO_2 , the crystalline sizes decreases after doping. the intensity was about the same peak observed all through except at 2% Ni-TiO_2 there observed a sharp decrease in intensity which also decreases the particles size thereby reduces the surface area of the photocatalyst as a results agglomeration of the catalyst.

Table 1a. XRF Result for 0.5% Ni-TiO_2 and 1% Ni-TiO_2

Element	Concentration (mg/Kg)		Percentage (%)	
	0.5% Ni-TiO_2	1% Ni-TiO_2	0.5% Ni-TiO_2	1% Ni-TiO_2
Mg	174.05	143.462	0.057941444	0.04556564
Al	1664.822	1551.769	0.554221144	0.492864648
Si	189.766	134.382	0.063173318	0.042681699
P	262.092	292.135	0.087250726	0.092786371
S	233.194	229.048	0.077630549	0.072749012
Cl	21.657	29.452	0.00720964	0.009354388
Ca	141.68	149.216	0.047165434	0.047393195
Ti	295832.154	307392.122	98.48286164	97.63225704
V	0	880.987	0	0.279814423
Mn	29.752	22.83	0.009904475	0.007251144
Fe	117.906	132.809	0.039251042	0.042182091
Ni	1667.432	3840.243	0.555090016	1.219717634
Mo	54.973	48.432	0.018300574	0.015382715
Total	300389.478	314846.887	100	100

Table 1b. XRF Result for 1.5% Ni-TiO_2 and 2% Ni-TiO_2

Element	Concentration (mg/Kg)		Percentage (%)	
	0.5% Ni-TiO_2	1% Ni-TiO_2	0.5% Ni-TiO_2	1% Ni-TiO_2
Mg	253.283	194.156	0.081510988	0.063173445
Al	1688.383	1629.816	0.543351771	0.530300847
Si	149.496	168.489	0.04811048	0.054822053
P	333.432	272.085	0.107304366	0.088529568
S	278.625	239.545	0.089666496	0.077941876
Cl	29.398	20.795	0.009460801	0.006766166
Ca	147.462	140.757	0.047455902	0.045798763
Ti	302308.667	297525.876	97.28832233	96.80738435
V	0	738.576	0	0.240313924
Mn	27.725	20.284	0.0089224	0.0065999
Fe	95.104	112.983	0.030606164	0.036761807
Ni	5381.827	6235.492	1.731967942	2.028871165
Mo	41.391	39.143	0.013320362	0.012736141
Total	310734.793	307337.997	100	100

Table 1a and 1b is the X-ray fractometry (XRF) of the synthesized photocatalyst, which displays elemental composition of the Ni-TiO_2 are express in percentage which confirms the presences of Nickel in percentage require abundance of titanium dioxide. However the results also reveals other element are present but in a negligible trace amount which can be attributed to two basic factor responsible. The most fundamental reason could be impurities occur during manufacturing process and second could be during weighing or synthesis.

Table 2a. Band gap energy of the synthesize catalysts

Catalyst	Wavelength (nm)	Band gap energy (ev)
0.5% Ni-TiO2	380	3.17
1% Ni-TiO2	400	3.09
1.5% Ni-TiO2	410	3.02
2% Ni-TiO2	420	2.95

Table 2a displays Band gap energy of the synthesized photocatalysts which were obtain spectrophotometrically. From the results obtained, there was a decrease in the band gap energy as the dopant increases and the wavelength increase thereby causes Red shift from Uv region to the visible region enabling photocalyst to harness visible to mineralize dye molecules.

Figure 1, 2, 3 and 4 shows the scan electron microscopy of the synthesized catalyst. From the result obtained indicates various morphology with their average pore sizes 15.4 μm^2, 11.6 μm^2, 9.4 μm^2 and 8.24 μm^2 respectively.

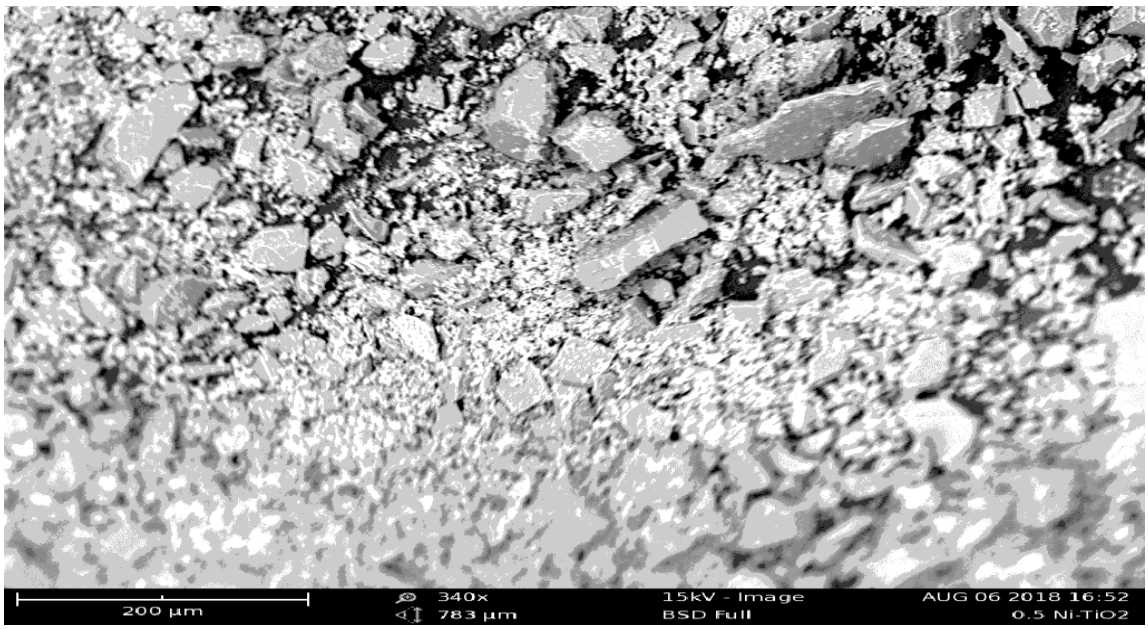

Figure 1. Scan electron microscopy of 0.5% Ni-TiO_2

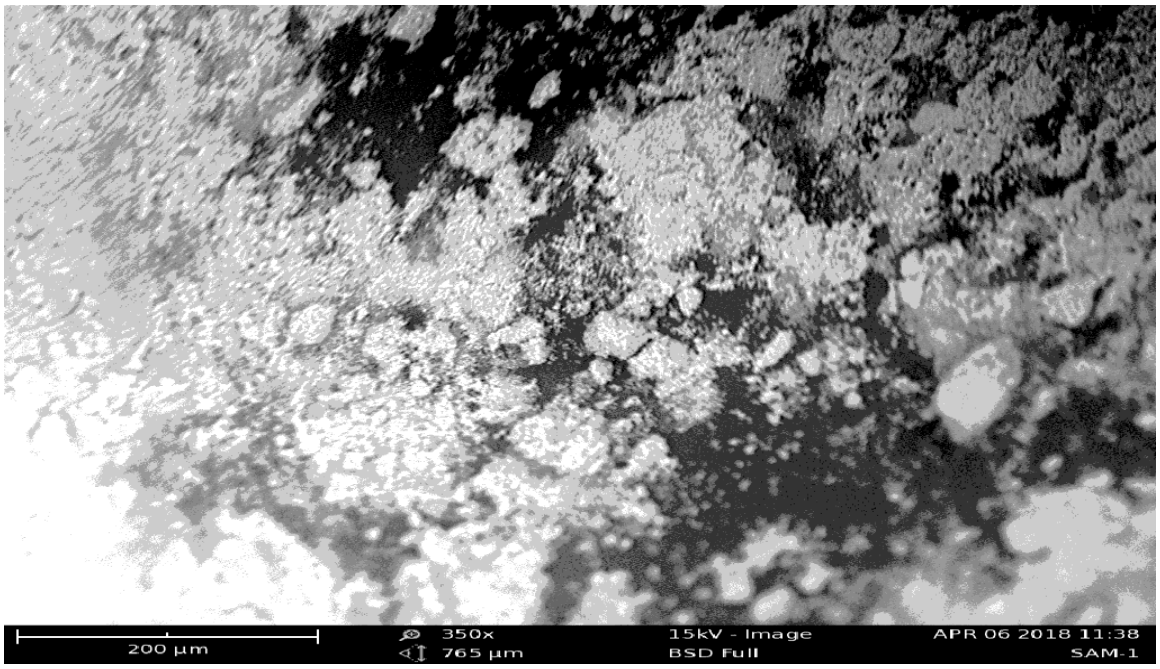

Figure 2. Scan electron microscopy of 1% Ni-TiO_2

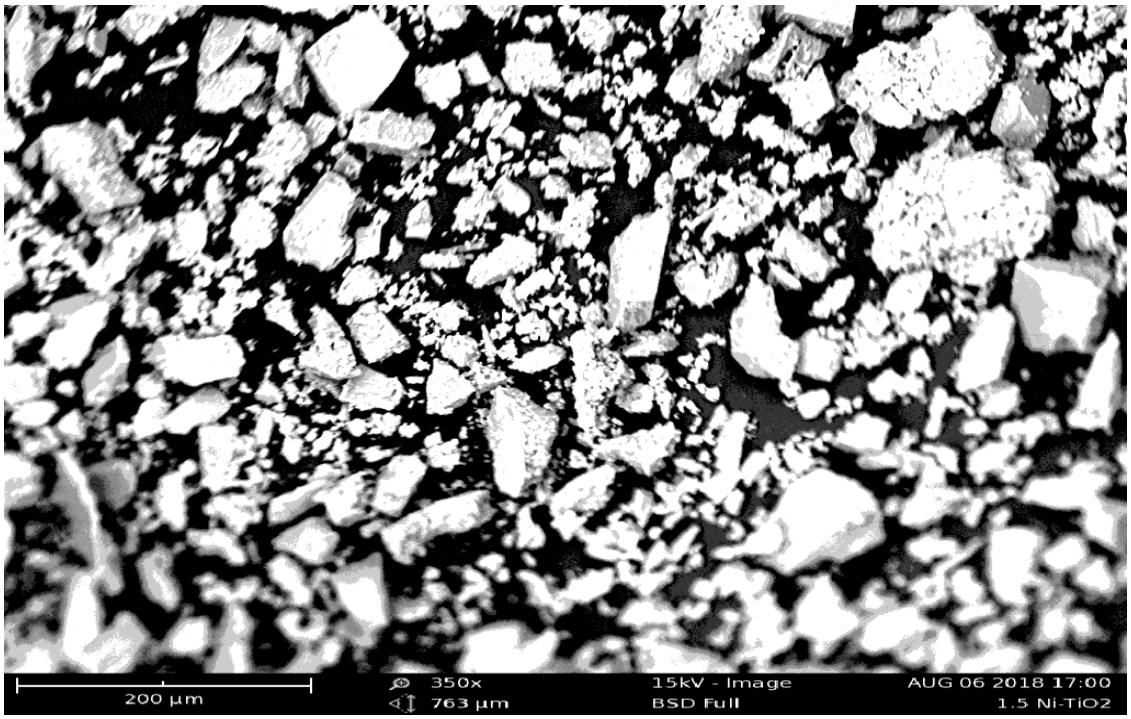

Figure 3. Scan electron microscopy of 1.5% Ni-TiO_2

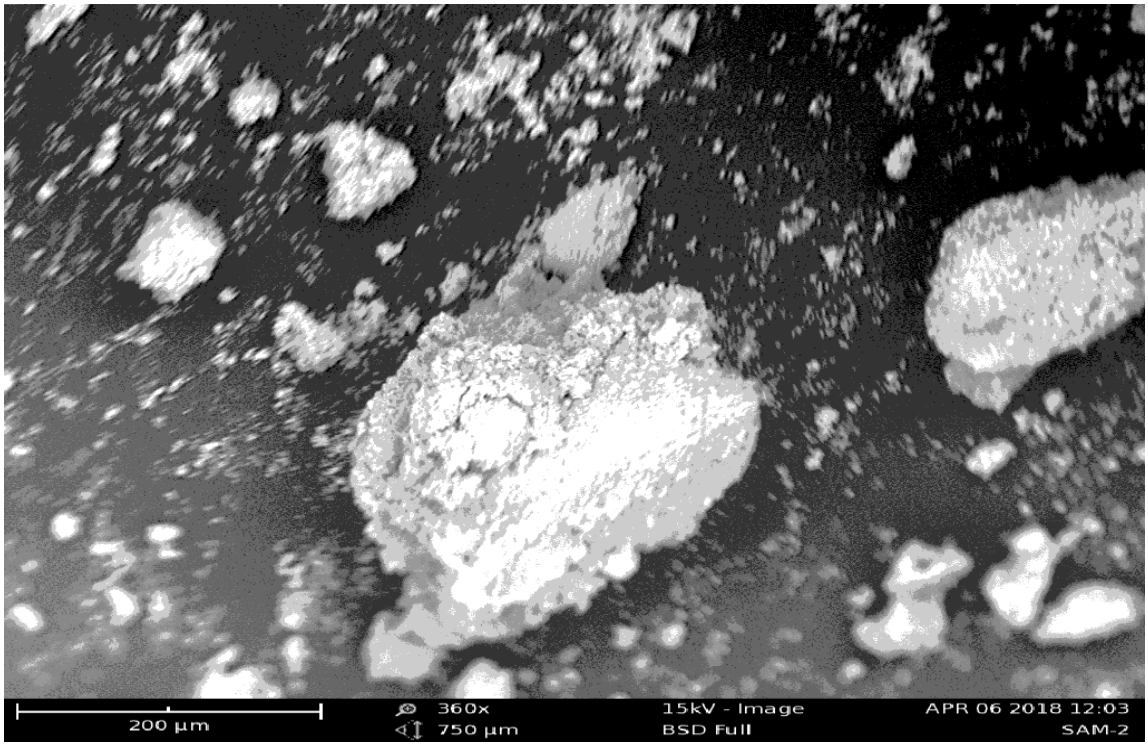

Figure 4. Scan electron microscopy of 2% Ni-TiO_2

Table 3a, 3b, 3c and 3d is showing the variation of % Degredation with respect to pH and irradiation time. It is evident that as the irradiation time increases there is a steady increase in degradation. Also, as the pH increases, the degradation also increases. This increase in % degradation as a result of increase in pH in alkaline region is attributed to the fact that more hydroxyl radicals were generated as a result of the reaction between hydroxyl ions and positive holes of the photocatalyst thereby increasing the rate of photodegradation. This is in agreement with a finding of (Akpan and Hameed, 2009, Tang and An, 1995, Goncalves, *et al.,* 1991).

It is worthy of mention that in an alkaline solution there exist coulombic repulsion between the negatively charge

surface of the photocatalyst and the hydroxide anion at a higher pH and this could prevent the formation of ·OH in higher alkaline solution thus decreasing the rate of photocatalytic degradation of the dye molecule (Akpan and Hameed, 2009).

Effect of pH and catalyst loading at a dye concentration 0.0001mol/dm^3 and irradiation time of 60 minutes. Changes in pH can influence the absorption of dye molecule on the surface of TiO_2 which is an important step for photocatalytic oxidation to take place (Fox and Dulay, 1993). The percentage degradation therefore increases as the pH moves toward the alkaline region. This is because in an acidic media, the TiO_2 particle aggnolomerate thereby reducing the surface available for dye absorption and photon absorption (Fox and Dulay, 1993) while the alkaline media favours the generation of more hydroxyl radical by oxidizing more hydroxyl ion on the surface of the photocatalyst thereby enhancing the efficiency of the photocatalyst (Goncalves, *et al.,* 1999) it then implies that percentage degradation greater than 95 is achievable at a pH of 5-9 and the catalyst loading of 0.5(g).

However percentage degradation in respect to irradiation time and the catalyst loading. An increment in irradiation time increases the rate of degradation as seen in the table above. Beyond certain time the rate of degradation could be affected negatively as a result of the short lifespan of the photocatalyst by active sites deactivation due to strong byproduct deposition. The catalyst loading also has an influence on the degradation rate. As the catalyst loading increases from 0.1-0.5, there was a progressive increase with a rate of reaction as shown in the aforementioned table. This increment is attributed to the fact that increase in the amount of the photocatalyst increases the number of the active sites on the photocatalyst surface which in turn increases the number of hydroxyl and superoxide radicals both of which are predominant species of degradation of dyes (Konstaninou and Albanis, 2004, Saquid and Muneer, 2008, Sun *et al.,* 2010; Liu *et al.,* 2006). This is true for dye concentration of 0.0000505 mol/dm^3 and a pH of 7 while it is 0.0000505mol./dm^3 and pH 7 at an irradiation time of 60 minutes.

Table 3a. Summary of a % Degradation for 0.5% Ni-TiO_2

Run Order	Catalyst Load (g)	pH	Time (min)	Dye Concentration (mol./dm3)	% Degradation
1	0.3	7	30	0.0000505	53.33
2	0.3	7	60	0.0001	61.54
3	0.3	5	30	0.000001	66.00
4	0.5	9	30	0.0000505	96.67
5	0.1	9	30	0.0000505	26.67
6	0.5	7	30	0.0001	60.00
7	0.3	7	60	0.000001	66.67
8	0.3	7	0	0.000001	0
9	0.3	5	0	0.0000505	0
10	0.3	9	60	0.0000505	98.50
11	0.5	7	60	0.0000505	94.56
12	0.1	7	0	0.0000505	0
13	0.1	7	60	0.0000505	33.33
14	0.3	7	0	0.0001	0
15	0.3	7	30	0.0000505	96.81
16	0.3	9	30	0.000001	77.78
17	0.3	7	30	0.0000505	50.00
18	0.3	7	30	0.0000505	53.33
19	0.5	7	30	0.000001	75.00
20	0.1	5	30	0.0000505	65.22
21	0.5	7	0	0.0000505	0
22	0.5	5	30	0.0000505	14.29
23	0.3	5	60	0.0000505	92.06
24	0.3	9	30	0.0001	97.71
25	0.1	7	30	0.0001	26.92
26	0.3	5	30	0.0001	73.33
27	0.1	7	30	0.000001	73.33
28	0.3	9	0	0.0000505	0

Table 3b. Summary of a % Degradation for 1% Ni-TiO_2

Run Order	Catalyst Load (g)	pH	Time (min)	Dye Concentration (mol./dm3)	% Degradation
1	0.3	7	30	0.0000505	84.71
2	0.3	7	60	0.0001	47.69
3	0.3	5	30	0.000001	87.50
4	0.5	9	30	0.0000505	95.27
5	0.1	9	30	0.0000505	22.73
6	0.5	7	30	0.0001	70.00
7	0.3	7	60	0.000001	87.08
8	0.3	7	0	0.000001	0
9	0.3	5	0	0.0000505	0
10	0.3	9	60	0.0000505	98.18
11	0.5	7	60	0.0000505	98.75
12	0.1	7	0	0.0000505	0
13	0.1	7	60	0.0000505	10.00
14	0.3	7	0	0.0001	0
15	0.3	7	30	0.0000505	85.71
16	0.3	9	30	0.000001	90.43
17	0.3	7	30	0.0000505	84.71
18	0.3	7	30	0.0000505	84.71
19	0.5	7	30	0.000001	91.67
20	0.1	5	30	0.0000505	12.12
21	0.5	7	0	0.0000505	0
22	0.5	5	30	0.0000505	98.53
23	0.3	5	60	0.0000505	92.42
24	0.3	9	30	0.0001	17.17
25	0.1	7	30	0.0001	26.15
26	0.3	5	30	0.0001	37.50
27	0.1	7	30	0.000001	75.00
28	0.3	9	0	0.0000505	0

Table 3c. Summary of a % Degradation for 1.5% Ni-TiO_2

Run Order	Catalyst Load (g)	pH	Time (min)	Dye Concentration (mol./dm3)	% Degradation
1	0.3	7	0	0.000001	0
2	0.3	9	0	0.0000505	0
3	0.1	7	0	0.0000505	0
4	0.3	7	30	0.0000505	98.88
5	0.3	7	60	0.000001	75.21
6	0.5	7	0	0.0000505	0
7	0.5	7	60	0.0000505	99.00
8	0.1	7	30	0.0001	61.54
9	0.3	9	30	0.0001	92.86
10	0.3	9	30	0.000001	66.67
11	0.3	7	60	0.0001	95.71
12	0.5	7	30	0.000001	54.55
13	0.3	7	0	0.0001	0
14	0.3	5	30	0.000001	50.00
15	0.3	7	30	0.0000505	98.88
16	0.5	9	30	0.0000505	99.00
17	0.3	7	30	0.0000505	98.88
18	0.5	7	30	0.0001	98.00
19	0.1	7	30	0.000001	58.33

Run Order	Catalyst Load (g)	pH	Time (min)	Dye Concentration (mol./dm3)	% Degradation
20	0.3	5	60	0.0000505	96.43
21	0.1	9	30	0.0000505	94.00
22	0.3	5	30	0.0001	99.17
23	0.3	7	30	0.0000505	98.88
24	0.3	9	60	0.0000505	99.00
25	0.1	5	30	0.0000505	94.00
26	0.5	5	30	0.0000505	99.00
27	0.3	5	0	0.0000505	0
28	0.1	7	60	0.0000505	97.00

Table 3d. Summary of a % Degradation for 2% Ni-TiO_2

Run Order	Catalyst Load(g)	pH	Time (min)	Dye Concentration (mol./dm3)	% Degradation
1	0.3	7	0	0.000001	0
2	0.3	9	0	0.0000505	0
3	0.1	7	0	0.0000505	0
4	0.3	7	30	0.0000505	84.71
5	0.3	7	60	0.000001	87.08
6	0.5	7	0	0.0000505	0
7	0.5	7	60	0.0000505	98.75
8	0.1	7	30	0.0001	26.15
9	0.3	9	30	0.0001	17.17
10	0.3	9	30	0.000001	90.43
11	0.3	7	60	0.0001	47.69
12	0.5	7	30	0.000001	91.67
13	0.3	7	0	0.0001	0
14	0.3	5	30	0.000001	87.50
15	0.3	7	30	0.0000505	85.71
16	0.5	9	30	0.0000505	95.27
17	0.3	7	30	0.0000505	84.71
18	0.5	7	30	0.0001	70.00
19	0.1	7	30	0.000001	75.00
20	0.3	5	60	0.0000505	92.42
21	0.1	9	30	0.0000505	22.73
22	0.3	5	30	0.0001	37.50
23	0.3	7	30	0.0000505	84.71
24	0.3	9	60	0.0000505	98.18
25	0.1	5	30	0.0000505	12.12
26	0.5	5	30	0.0000505	98.53
27	0.3	5	0	0.0000505	0
28	0.1	7	60	0.0000505	10.00

The effect of irradiation time and dye concentration at a catalyst loading of 0.5(g) and a pH of 7. It is evident that as the irradiatin time increases there is a corresponding increase in the % degradation. Photocatalytic degradation also increases with increase in the dye concentration and this may be attributed to the fact that as the dye concentration increases, more dye molecules become available foe excitation for energy transfer, resulting in an increase in rate of reaction. But beyond a concentration of 0.0001mol./dm^3, increases in the concentration of the dye molecules may acts as a blanket or cover and will not permit the desired light intensity to reach the semiconductor surface. Thus, decreasing the rate of photocatalysis (Davi *et al.*, 1994).

Effect of pH and dye concentration for a catalyst loading of 0.3 and irradiation time of 30 minutes. The percentage degradation increases as the pH increases from neutral to alkaline region and this can be as a result of the availability of hydroxide ion in pH range of 5-9 which combine with holes formed due to electron excitation of the catalyst. This is in agreement with the finding (Akpan and Hameed, 2009

and Konstaninou and Albanis, 2004,) that the rate of degradation is higher at alkaline pH because alkaline pH favours the generation of the hydroxyl radicals which enhances the rate of photodegradation (Sun *et al.,* 2010, Baran *et al.,* 2008, Xiao *et al.,* 2007) as the concentration also increases the rate of degradation also increases as seen from the plot.

Interraction between catalyst load and dye concentration on the rate of degradation. The amount of the photocatalyst is one of the most important parameter that affects the rate of photocatalytic degradation of organic colorants. The effects of variation in the amount of photocatalyst from 0.1-0.5g and concentration of dye and at pH of 7 and irradiation time of 30 minutes were measured. On the rate of degradation, it was found that catalyst loading increases, the rate of degradation also increases. Increase in the rate of degradation with increase in the amount of catalyst is due to the availability of more catalyst surface area for absorption of photons of light and interaction of molecules of reaction mixture with catalyst, with resultant increase in the number of holes, hydroxyl radical and super oxide ions (O_2^- . As the dye concentration is increased from 0.000001mol./dm^3 to 0.0001mol./dm^3 the number of dye molecule in the solution also increases with corresponding increase in the percentage degradation (Akpan and Hameed, 2009, Sun *et al.,* 2010; Liu *et al.,* 2006).

4. Conclusions

1. At the end of this research work, we have successfully developed Ni-TiO_2 through wet impregnation rout that is markedly enhance the absorption of visible photocatalytic degradation of wastewater from tannery containing acid azo dyes.
2. Crystalline structure of Ni-dopedTiO_2 exhibit anatase-type crystallite, determined from XRD analysis. In UV absorption spectra, the absorption edge Ni-TiO_2 shows a shift to visible-light region, followed by an ovious absorption peak at 400-420 nm this transformation can be ascribed to the formation of impurities energy level within the band gap, improving the visible-light photocatalysis of dye tannery wastewater.
3. Visible-light photocatalysis capacities are increasing function from 0.5% Ni-TiO_2, 1% Ni-TiO_2, 1.5% Ni-TiO_2 and 2% Ni-TiO_2. The pore size of the catalyst may play a major factor in removing the dye form aqueous solution.

ACKNOWLEDGMENTS

The Authors wishes to express their profound gratitude to Umaru Musa State university, Katsina state Nigeria for carrying out the Scan Electron Microscopy (SEM) and X-Ray Diffraction (XRD) and Ahmadu Bello Univrsity Zaria for carrying out X-Ray fractometer and Band-gap energy analysis.

REFERENCES

[1] Arshlan-Alaton (2007). Degradation of commercial textile biocide with Advanced Oxidation Processes and Ozone. J. Environ Manag. 82(2), 145-154.

[2] Visinescu C. M, Sanjines R., Levy F, and Parvulescu V. I. (2005) "Photocatalytic degradation of acetone by Ni-doped titania thin films prepared by dc reactive sputtering," Appl. Catal. B- Environmental, vol. 60, no. 3–4, pp. 155–162, 2005.

[3] Forgacs E, Cserhati T, Oros G (2004) Removal of synthetic dyes from wastewaters: a review. Environ Int 30: 953–971.

[4] Ganesh, I., Gupta A.K., Kumar, P.., Sekhar, P.S.C., Radha, K., Padmanabham, G. and Sundararajan, G. 2012. "Preparation and characterization of Ni-doped TiO_2 materials for photocurrent and photocatalytic applications", Science World journal, in press.

[5] Gomathi DL, Girish KS, Mohan RK, Munikrishnappa C (2009) Photo degradation of methyl orange an azo dye by advanced Fenton process using zero valent metallic iron: influence of various reaction parameters and its degradation mechanism. J Hazard Mater 164: 459–467.

[6] Han F, Kambala VSR, Srinivasan M, Rajarathnam D, Naidu R (2009) Tailored titanium dioxide photocatalysts for the degradation of organic dyes in wastewater treatment: a review. Appl Catal A 359: 25–40.

[7] Liu, X.H., He, X.B., Fu, Y.B. 2008. Effects of doping cobalt on the structures and performances of TiO_2 photocatalyst, Acta Chimica Sinica, 66 1725–1730.

[8] Ahmed M. A. (2012). "Synthesis and structural features of mesoporous NiO/TiO_2 nanocomposites prepared by sol–gel method for photodegradation of methylene blue dye," J. Photochem. Photobiol. A Chem., vol. 238, no. 0, pp. 63–70, 2012.

[9] Ahmed M. A., El-Katori E. E., and Gharni Z. H. (2018) "Photocatalytic degradation of methylene blue dye using Fe2O3/TiO2 nanoparticles prepared by sol–gel method," J. Alloys Compd., vol. 553, pp. 19–29, 2013.

[10] Martı´nez Huitle CA, Brillas E (2009) Decontamination of wastewaters containing synthetic organic dyes by electrochemical methods: a general review. Appl Catal B 87: 105–145.

[11] O ¨zcan A, Oturan MA, Oturan N, Sahin Y (2009). Removal of acid orange 7 from water by electrochemically generated Fenton's reagent. J Hazard Mater 163:1213–1220.

[12] Pouran S.R, Aziz A.A, David W.M.A.W, Shafeeyan M.S (2015). Effect of Niobium and Molybdenum impregnation on adsorption capacity and fenton catalytic activity of magnetic RSC Adv. 5(106), 87535-87549.

[13] Rawal S.B, Ojha D.P, Choi Y.S, Lee W.I (2014). Coupling of W-doped SnO_2 and TiO_2 for effluent visible-light photocatalysis. Bull Korean Chem Soc. 35(3), 913-918.

[14] Yan-Hua Peng, Gui-Fang Huang, Wei-Qing Huang (2012). Visible-light absorption and photocatalytic activity of Cr-doped TiO_2 nanocrystal films. International journal of Advanced powder Technology, 23(1) 8-12.

[15] Zhang W, Yang B, Chen J (2012). Effect of calcination temperature on preparation of boron doped TiO_2 by sol-gel method. Int. J. Photoenergy.

[16] Akpan, U.G. and Hameed, B.H., (2009). Parameters affecting the photocatalyti degradation of dyes using TiO_2-based photocatalysis: A review, *joural of Hazardeous material*, 170 pp 520-529.

[17] Baran, W., Makowski, A., Wardas, W (2008). The effect of Uv radiation absorption of cationic and anionic dye solutions on their photocatalytic degradation in the presence of TiO_2, dyes pigment. 76; pp 226-230.

[18] Xiao, Q. Zhang, J. Xiao, C. Si, Z. and Tan, X. (2008). Solar photocatalytic degradation of methylene blue in carbon-doped TiO_2 nanoparticles suspension," *Solar Energy*, vol. 82, no. 8, pp. 706–713.

[19] Akpan, U.G. and Hameed, B.H., (2009). Parameters affecting the photocatalytic degradation of dyes using TiO_2-based photocatalysis: A review, *joural of Hazardeous material*, 170 pp 520-529.

[20] Fox, M.A and Dulay, M.T. (1993). Heterogeneous photocatalysis. Chemistry. Reviewed. 93; pp 341-357.

[21] Goncalves, M.S.T., Oliveira-Campos, A.M.F., Pinto, E.M.M.S., Plasencia, P.M.S., Queiroz, M.J.R.P. (1999). Photochemical treatment of solution of azo dyes containing TiO_2. Chemosphere 39, pp. 781-786.

[22] Tang, W.Z. An, H. (1995). Photocatalytic degradation kinetics and mechanism of acidv blue 40 by TiO_2/UV in aqueous solution, Chemosphere 31pp 4171–4183.

[23] Konstantinou, K.I, and Albanis, T.A. (2004). "TiO_2-assisted photocatalytic degradation of azo dyes in aqueous solutions: Kinetic and mechanistic investigation n: A review; *Journal of applied catalysis* B: Environmental, vol. 49, pp. 1-14.

[24] Saquid, M., Muneer, M. (2008). Dyes pigments 56; pp. 49.

[25] Sun, H. Wang, S. Ang, H.M. Tad ́e, M.O. and Li, Q. (2010). Halogen element modified titanium dioxide for visible light photocatalysis, *Chemical Engineering Journal*, vol. 162, no. 2, pp. 437–447.

[26] Liu A. R., Wang, S. M. Zhao, Y. R. and Zheng, Z. (2006) "Lowtemperature preparation of nanocrystalline TiO_2 photocatalyst with a very large specific surface area," *Materials Chemistry and Physics*, vol. 99, no. 1, pp. 131–134, ISRN Materials Science 15.

[27] Baran, W., Makowski, A., Wardas, W (2008). The effect of Uv radiation absorption of cationic and anionic dye solutions on their photocatalytic degradation in the presence of TiO_2, dyes pigment. 76; pp 226-230.

[28] Akpan, U.G. and Hameed, B.H., (2009). Parameters affecting the photocatalytic degradation of dyes using TiO_2-based photocatalysis: A review, *joural of Hazardeous material*, 170 pp 520-529.

[29] Devi, L. G. Murthy, B. N. and Kumar, S. G. (2010). Photocatalytic activity of TiO_2 doped with Zn^{2+} and V^{5+} transition metal ions: influence of crystallite size and dopant electronic configuration on photocatalytic activity," *Materials Science and Engineering B*, vol. 166, no. 1, pp. 1–6.